

Designer amphiphilic proteins as building blocks for the intracellular formation of organelle-like compartments

Matthias C. Huber^{1,2,3,4†}, Andreas Schreiber^{1,2,3,5†}, Philipp von Olshausen^{6,7}, Balázs R. Varga⁸, Oliver Kretz⁷, Barbara Joch⁹, Sabine Barnert^{4,10}, Rolf Schubert^{4,7,10}, Stefan Eimer⁷, Péter Kele⁸ and Stefan M. Schiller^{1,2,3,4,5,7,11,12★}

Nanoscale biological materials formed by the assembly of defined block-domain proteins control the formation of cellular compartments such as organelles. Here, we introduce an approach to intentionally ‘program’ the *de novo* synthesis and self-assembly of genetically encoded amphiphilic proteins to form cellular compartments, or organelles, in *Escherichia coli*. These proteins serve as building blocks for the formation of artificial compartments *in vivo* in a similar way to lipid-based organelles. We investigated the formation of these organelles using epifluorescence microscopy, total internal reflection fluorescence microscopy and transmission electron microscopy. The *in vivo* modification of these protein-based *de novo* organelles, by means of site-specific incorporation of unnatural amino acids, allows the introduction of artificial chemical functionalities. Co-localization of membrane proteins results in the formation of functionalized artificial organelles combining artificial and natural cellular function. Adding these protein structures to the cellular machinery may have consequences in nanobiotechnology, synthetic biology and materials science, including the constitution of artificial cells and bio-based metamaterials.

Proteins combine exact sequence, and thus atomic composition, with well-defined three-dimensional (3D) structures. Hence, they are attractive candidates for the formation of functional nanoscale materials that require exact molecular composition and structure, for example, compartmentalized structures such as vesicular or micellar assemblies.

In biology, compartmentalization is a common concept and can be observed in the separation of anabolic and catabolic reactions, signal molecules and organizing multi-enzyme complexes within cells and multicellular organisms. Whereas eukaryotic cells contain intracellular compartments, termed organelles, prokaryotes lack this membrane-based compartmentalization. In prokaryotes, compartmentalized structures comprise enzyme complexes and bacterial microcompartments based on protein skeletons^{1,2}. These structures resemble virus capsid skeletons^{3,4} functionally restricted to a few pathways⁵, whereas membrane-based organelles within eukaryotic cells consist of dynamic membranes formed from amphiphilic phospholipid building blocks with a multitude of functions. Membrane-bound organelles are usually not formed *de novo*, however, but form from pre-existing organelles. The *de novo* constitution of a basic requirement of life, the

cellular compartment *in vitro* and *in vivo*, has been investigated extensively^{6,7}. The formation of protein-based spherical higher-order structures has been demonstrated *in vitro*^{8–11}. However, the ability to control the synthesis and assembly of specific molecular building blocks and their assembly to defined membrane-enclosed dynamic organelle-like structures *in vivo* is yet to be achieved.

The formation of lipid-enclosed organelles is based on a complex regulatory and synthetic network and cannot be realized at present to make new organelles *de novo*. Thus, concepts using an alternative class of amphiphilic molecules enabling the constitution of dynamic membranes need to be developed. The need to address this question is supported by the request for programmable organelles *in vivo* for medical and technological applications^{12–14}. Such systems could be applied to the synthesis of defined pharmaceuticals¹⁵ directly in the patient¹⁶. In addition, new organelles may have far reaching consequences in cell development and in expression of membrane proteins, and may aid in answering questions concerning the functional network of the cell.

Here, we report a synthetic biology approach to control the *de novo* formation of dynamic, membrane-enclosed compartments using genetically encoded amphiphilic block-domain proteins as

¹Institute for Macromolecular Chemistry, University of Freiburg, Stefan-Meier-Str. 31, D-79104 Freiburg, Germany. ²Institute for Pharmaceutical Sciences, University of Freiburg, Albertstr. 25, D-79104 Freiburg, Germany. ³Freiburg Institute for Advanced Studies (FRIAS), School of Soft Matter Research, University of Freiburg, Albertstr. 19, D-79104 Freiburg, Germany. ⁴Faculty of Chemistry and Pharmacy, University of Freiburg, Fahrenbergplatz, D-79104 Freiburg, Germany. ⁵Faculty of Biology, University of Freiburg, Schänzlestrasse 1, D-79085 Freiburg, Germany. ⁶Bio- and Nano-Photonics, Department of Microsystems Engineering, University of Freiburg, Georges-Köhler-Allee 102, D-79110 Freiburg, Germany. ⁷BIOSS Centre for Biological Signalling Studies, University of Freiburg, Schänzlestrasse 18, D-79104 Freiburg, Germany. ⁸Chemical Biology Research Group, Hungarian Academy of Sciences, CNS, IOC, Magyar tudósok krt. 2, H-1117 Budapest, Hungary. ⁹Institute for Neuroanatomy University of Freiburg, Albertstr. 17, D-79104 Freiburg, Germany. ¹⁰Institute of Pharmaceutical Sciences, Department of Pharmaceutical Technology and Biopharmacy, University of Freiburg, Hermann-Herder-Str. 9, D-79104 Freiburg, Germany. ¹¹IMTEK Department of Microsystems Engineering, University of Freiburg, Georges-Köhler-Allee 103, D-79110 Freiburg, Germany. ¹²Center for Biosystems Analysis (ZBSA), University of Freiburg, Habsburger Str. 49, D-79104 Freiburg, Germany. [†]These authors contributed equally to this work. ★e-mail: Stefan.Schiller@FRIAS.Uni-Freiburg.de

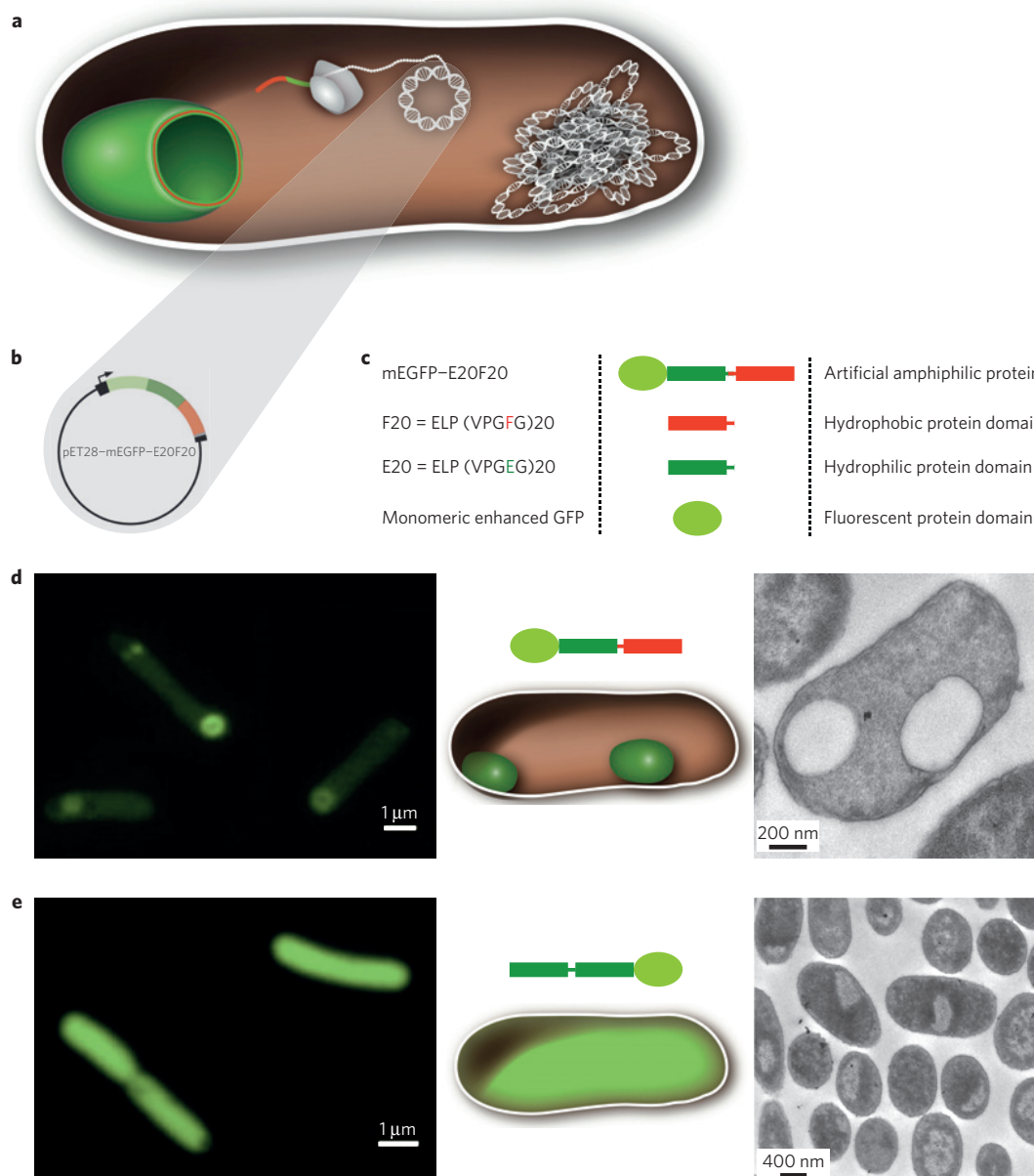


Figure 1 | The design and expression of artificial amphiphilic proteins with the potential for self-assembly allows the formation of cellular compartments in *E. coli*. **a**, A schematic overview of the recombinant expression and self-assembly of the amphiphilic block-domain proteins into cellular compartments *in vivo*. **b**, An illustration of the plasmid pET28-mEGFP-E20F20 encoding the depicted artificial amphiphilic protein (mEGFP-E20F20). **c**, The left panel shows the composition and abbreviations of the designated proteins. The middle panel illustrates the schematic symbols for the proteins. The right panel presents the properties for the functional assignment of the proteins forming organelle-like structures *in vivo*. **d**, The expression of amphiphilic mEGFP-E20F20 *in vivo* leads to the formation of compartments in *E. coli* visualized within living cells by epifluorescence microscopy (left panel). The right panel shows a fixed microtome slice of a single *E. coli* cell imaged using TEM. A schematic illustration of the respective artificial protein and the cellular compartments in *E. coli* is shown in the middle panel. **e**, The expression of the hydrophilic E40-mEGFP control proteins in *E. coli* visualized by epifluorescence microscopy exhibiting a uniform distribution of the protein in *E. coli* cells (left panel). The TEM image of a microtome slice of *E. coli* expressing E40-mEGFP does not show any compartmentalization (right panel). Bright areas inside the cell correspond to genomic DNA. The middle panel schematically illustrates the homogenic distribution of the control proteins in *E. coli*.

molecular building blocks (Fig. 1a–c). *In vivo* self-assembly of these nanoscale building blocks and their site-specific functionalization by genetically encoded unnatural amino acids results in the formation of artificial membrane-based organelles.

In this approach, the precise adjustment of the physico-chemical characteristics of the amphiphilic proteins is realized by the *de novo* generation of hydrophilic or hydrophobic homopolymeric protein domains, which can be genetically assembled to make amphiphilic block-domain proteins. For example, amphiphilicity and ‘lipid-like’

geometry (similar to phospholipids¹⁷ in cell membranes) can be tuned by varying the total length and ratio between hydrophilic and hydrophobic protein domains. It is known from phospholipids in cell membranes that the shape of the amphiphilic lipid determines its ability to form planar membranes or micellar structures. Structures that constitute ‘cylindrical’ molecular geometries are known to support the formation of planar bilayers in contrast to asymmetric geometries with conical shapes known to support the formation of micellar superstructures¹⁷. Geometrically controlled

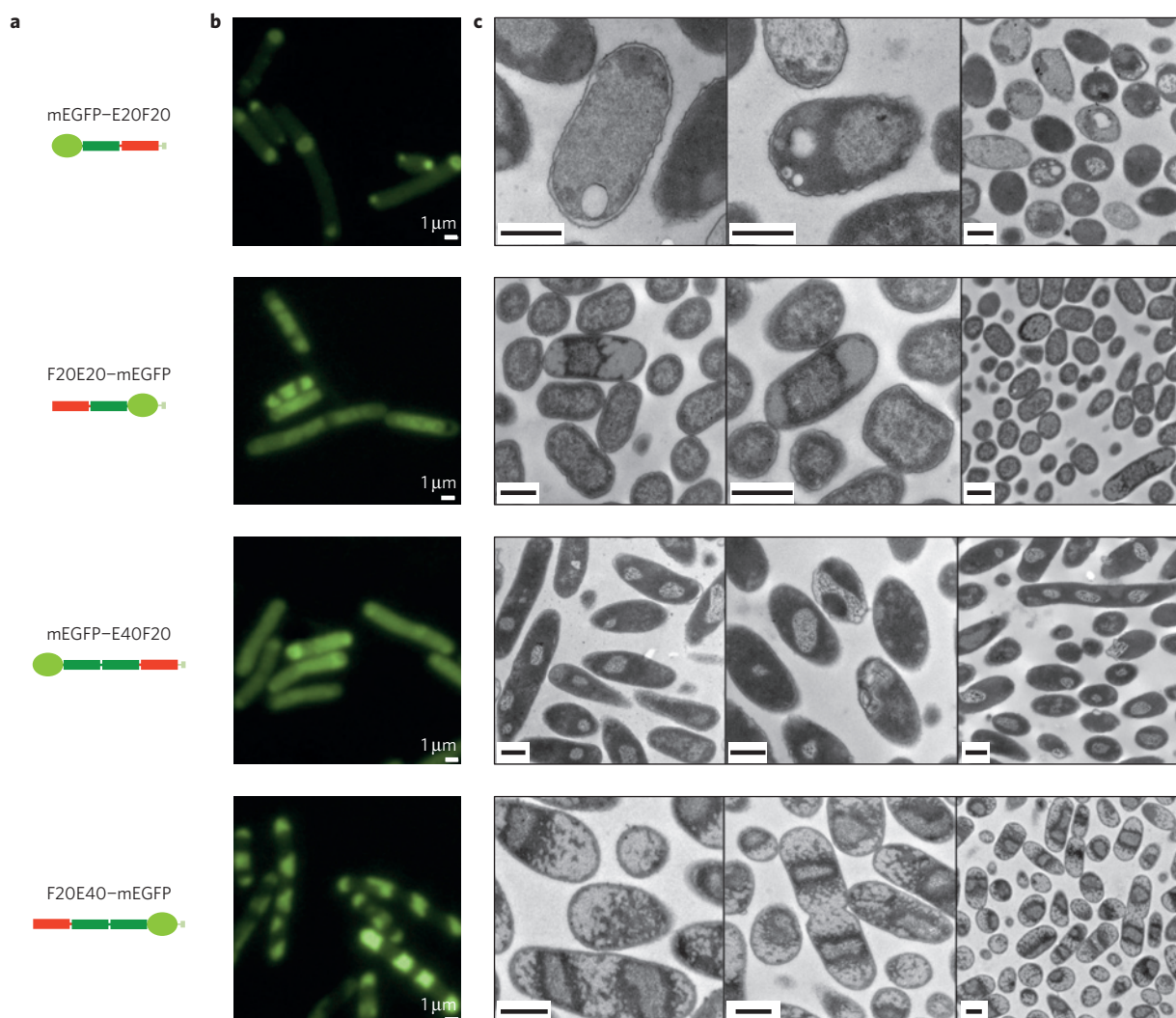


Figure 2 | The influence of the translational order and ratio of amphiphilic block domains on the subcellular distribution and higher-order structure formation *in vivo*. **a**, Notation and schematic illustration of the protein composition and orientation for respective rows in **b** and **c**. The light green circle indicates the mEGFP domain, the green rectangle the ELP-E20 protein domain (both hydrophilic) and the red rectangle the hydrophobic ELP-F20 domain. **b**, Epifluorescence images of *E. coli* expressing different *de novo*-generated amphiphilic proteins presented in **a**. Cells reveal an individual distribution pattern of the amphiphilic fluorescent proteins *in vivo* depending on the N- or C-terminal localization of the hydrophobic/hydrophilic protein domains and the ratio between the block domains. **c**, Corresponding TEM images of fixed *E. coli* cells (compare: **a,b**) confirm the *in vivo* findings (**b**). First row: *E. coli* cells expressing mEGFP-E20F20 form cellular compartments. Second row: the inverted arrangement of identical domains F20E20-mEGFP leads to a complete loss of the compartment-forming potential. A significant tendency to form different structures, for example, inclusion bodies or micellar complexes is shown. Third row: expression of mEGFP-E40F20 reveals the formation of complex mesh- or multilaminar compartment-like structures in *E. coli* that occasionally seem to interact with the cell membrane. Fourth row: the inverted construct F20E40-mEGFP shows precisely delimited areas of micellar protein localization and organization completely different from the inverted protein building blocks. The scale bars in the TEM images correspond to 0.5 μm .

structures such as the β -spirals^{18,19} of elastin-like proteins (ELPs) have been used *in vitro* to shape the global geometry of amphiphilic block-domain proteins in analogy to phospholipids. Resulting assemblies comprise micellar, tubular, vesicular or other higher-order structures *in vitro*^{9,11,20,21}. Thus, we aim to synthesize proteins with an amphiphilic ratio allowing the formation of membrane-like structures *in vivo*.

Our protein domains are derived from repetitive ELP amino-acid sequence motifs based on the VPGVG repeat unit, which is known to tolerate mutations at the fourth position (valine; V) whilst maintaining its structural and functional properties²². This variability permits the adjustment of the protein domain properties by changing the number of repeat units or the amino acid at the fourth position. The hydrophilic protein domain was modified with glutamic acid (E) at the fourth position of each

pentameric-repeating motif and with phenylalanine (F) at the same position for the hydrophobic domain. To monitor the expression, distribution and assembly of the resulting proteins within the living cell, they were supplemented with the fluorescent protein domain mEGFP at their hydrophilic end (Fig. 1b,c).

To study the influence of varying composition ratios of hydrophilic versus hydrophobic domains and their translational orientation on the spatial distribution and self-organization potential *in vivo*, we generated (for details, see Supplementary Information) a set of artificial proteins and investigated their subcellular behaviour (Fig. 1b–e). The amphiphilic block-domain protein mEGFP-E20F20 consisting of twenty units of VPGEG and twenty units of VPGFG proved to be very efficient in forming organelle-like structures *in vivo*. The plasmid containing the DNA sequence of the amphiphilic protein was created by a modified

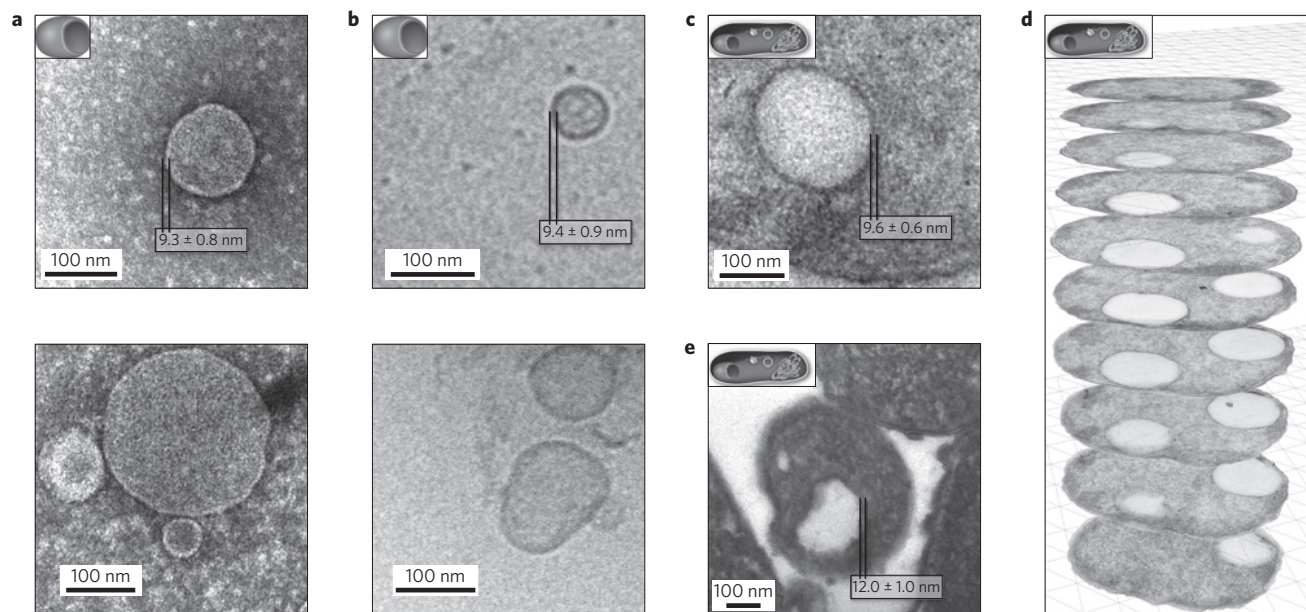


Figure 3 | The self-assembly of mEGFP-E20F20 proteins to form vesicular-like structures *in vitro* and *in vivo* visualized by cryo-TEM, HPF- and conventional TEM. Vesicular-like structures with dimensions ranging from approximately 40 nm up to a few hundred nanometres in diameter. Membrane thicknesses of these structures were measured (Supplementary Data 3). Values are presented in the upper panel of each part of the figure as well as schematic symbols of the spherical structure *in vitro* or *in vivo*. **a**, Conventionally stained TEM images of *in vitro*-assembled, his-tag purified amphiphilic mEGFP-E20F20 proteins. The purified protein alone is able to form vesicular structures. **b**, *In vitro*-assembled, cryo-fixed and TEM-imaged vesicular structures confirm the vesicular structures presented in **a**. **c**, The *in vivo* formation of cellular compartments was imaged using conventional TEM. **d**, TEM images of a z-stack of 55-nm-thick conventionally fixed and stained slices of *E. coli* cells expressing the artificial amphiphilic protein mEGFP-E20F20. The 3D composition of the individual images visualizes the spherical arrangement of the cellular compartments constituted *in vivo*. **e**, The *in vivo* formation of cellular compartments was imaged using HPF-TEM to confirm the findings of conventionally fixed TEM (Supplementary Methods). The measured apparent membrane thicknesses of the vesicular/compartment-like structures for all presented fixation techniques *in vitro* and *in vivo* are comparable.

cloning approach (see Methods and Supplementary Information) and transformed into *E. coli* cells (*BLR* strain, ER2566 strain; Fig. 1b) for protein expression and subsequent organelle formation. After inducing expression of the amphiphilic block-domain protein, cells were allowed to express the artificial protein for various time frames and imaged with epifluorescence microscopy and transmission electron microscopy (TEM). In Fig. 1d vesicular fluorescent objects can be observed in almost every cell (see also Supplementary Fig. 1a). These fluorescent higher-order structures indicate the formation of spherical structures surrounded by a membrane consisting of the fluorescent protein mEGFP-E20F20 as illustrated in Fig. 1d (middle panel).

To confirm the vesicular nature of these *de novo* organelles, *E. coli* cells were grown for 7–8 h after induction of protein expression and fixed. Microtome slices (55 nm thick) were prepared and analysed using TEM. The images in Fig. 1d (right panel) prove the presence of artificial organelles represented by hollow structures in the range of approximately 500 nm surrounded by a clearly visible membrane composed of the amphiphilic protein as seen in the epifluorescence images. In contrast, hydrophilic control proteins E40-mEGFP and E60-mEGFP expressed under the same conditions do not form such artificial organelles and equally distribute within the cell (Fig. 1e and Supplementary Fig. 1b and Table 1a,b).

By changing the ratio of hydrophilic versus hydrophobic protein domain length it could be shown that only a very narrow range of ratios allows for the assembly of organelle-like structures (Figs 1d and 2 and Supplementary Fig. 7b). This supports an interaction mechanism comparable to phospholipids. Asymmetric ratios of hydrophilic versus hydrophobic protein (for example, mEGFP-E40F20) domains rapidly result in a loss of the ability to form artificial organelles. Furthermore, TEM images of cells expressing mEGFP-free amphiphilic proteins with the

corresponding hydrophilic versus hydrophobic ratio show that artificial organelle formation does not depend on the mEGFP-tag (Supplementary Table 1c). In addition, it is known that the orientation of hydrophilic or hydrophobic domains at the amino or carboxy terminus of proteins²³ influences the structural and functional properties of proteins. Confirming these findings we show that the translational order of the protein domains (hydrophobic or hydrophilic first) influences the self-assembly process and the structures formed (Fig. 2 and Supplementary Fig. 7a). Expressing constructs with identical hydrophilic versus hydrophobic protein compositions but different translational order (N to C terminus) results in different morphologies formed within the living cell (Fig. 2 and Supplementary Figs 4b and 7a). In contrast, non-amphiphilic protein constructs show a behaviour independent of the translational order and exhibit homogeneous protein distributions *in vivo* (Supplementary Table 1a,b). On a molecular basis the variations of the resulting structures can be explained by the folding processes occurring at the ribosomal exit tunnel²⁴. If the hydrophilic part is translated first, the peptide chain is hydrated in the cytoplasm before the hydrophobic domain is translated. Thus, intra- and intermolecular interaction effects in the cytoplasm facilitate a certain structure formation different from the hydrophobic domain. If the hydrophobic domain of the peptide is expressed first it undergoes hydrophobic interactions within the same molecule or cytoplasmic components, changing folding and supramolecular structure formation. Thus, translational order and ratio of hydrophilic versus hydrophobic protein domains are important factors influencing the self-assembly process into artificial organelles *in vivo*.

The 3D structure of the protein-based membrane of the organelle was confirmed by preparing a z-stack series of 55-nm-thick microtome slices of embedded *E. coli* cells. The slices were

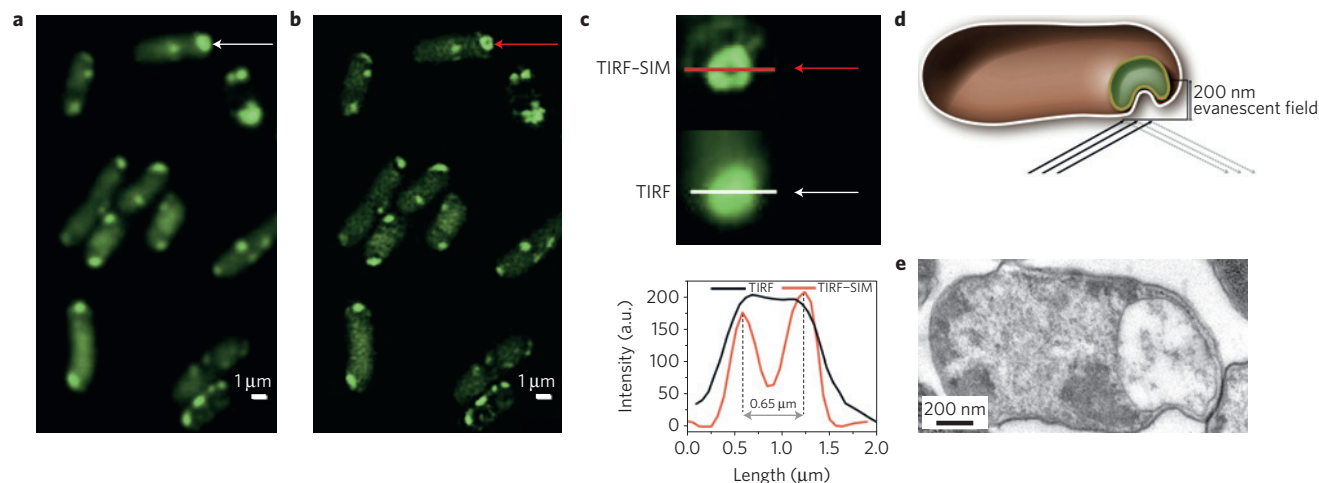


Figure 4 | TIRF and TIRF-SIM fluorescence microscopy images resolve the structure of the artificial cellular compartments in *E. coli* cells. **a, TIRF fluorescence image of living *E. coli* cells. **b**, TIRF-SIM fluorescence imaging of living *E. coli* cells enhances the resolution and elucidates detailed structural characteristics of the compartment-like structures. **c**, Line scans of TIRF-SIM (**b**) and TIRF images (**a**). **d**, Schematic picture of an invaginating cellular compartment investigated using TIRF and TIRF-SIM. **e**, TEM-imaged microtome slice of *E. coli* (55 nm in width).**

investigated by conventional TEM (Fig. 3d). The TEM images prove the spherical structure of the artificial *de novo* compartments. One or more organelle-like compartments were observed to be inside a cell. The images show the stained amphiphilic protein membrane surrounding and separating the lumen of the artificial compartments from the cytoplasm and the 3D spherical shapes of the artificial organelles inside the cell (Fig. 3d). These findings demonstrate an efficient and defined self-assembly process and a strong directional interaction of the designed protein building blocks *in vivo*.

Analysis of the inner composition of the compartments *in vivo* was performed by element-specific imaging analysis for the elements N and P and high-contrast imaging with scattered electrons on microtome slices. All measurements show the same composition for the organelle-like interior as for the embedding environment around the cells strongly indicating 'empty', water-filled compartment-like structures without significant protein- or heteroatom-containing molecules inside the compartment *in vivo*. Conventional TEM fixation using glutaraldehyde and subsequent dehydration at room temperature can lead to artefacts, which occasionally result in structures resembling vesicles. To overcome this problem we applied high-pressure freeze (HPF) solvent-substitution TEM (see Supplementary Methods), which results in a close-to-native ultrastructural preservation^{25–27}. Applying this alternative approach we found vesicles of the same size and membrane dimensions and with the same ultrastructural characteristics as observed after conventional TEM fixation (Fig. 3 and Supplementary Fig. 4).

To address the question of whether the amphiphilic protein by itself is sufficient to form artificial organelles *in vivo*, we expressed and purified the protein (Supplementary Fig. 2) and investigated its ability to self-assemble into vesicular structures *in vitro*. *In vitro* vesicle assembly was proven using TEM and cryo-TEM (Fig. 3a,b). This demonstrates the ability of the pure, newly designed amphiphilic protein to form vesicular structures without any other constituents. Further, amphiphilic-protein-based vesicle formation *in vitro* could be shown at conditions comparable to the intracellular environment of *E. coli*. Vesicle formation of amphiphiles, such as fatty acids, occurs most efficiently around their pK_a (ref. 28) but is also dependent on osmolarity (OsM), solvent, temperature and cooperative effects. *In vitro*, assembly of our amphiphilic proteins was performed at 0.5 OsM and across a broad pH range (from 7.5 to 9.2) at room temperature. These

in vitro conditions can be compared to the formation process *in vivo*, which is influenced by intracellular conditions of *E. coli* (pH around 7.6 (ref. 29), osmolarity about 0.3 OsM (ref. 30) and temperature of 20 °C). Vesicular organization of amphiphiles, for example fatty acids, causes important cooperative effects leading to tremendous pK_a shifts (from 4.5 to 8.5 for oleic acid as a result of the close packing of the carboxyl groups in the shell of the vesicle) affecting the self-assembly process^{28,31}. Hence *in vitro* and *in vivo* assembly could be achieved at comparable environmental conditions.

For real-time analysis of artificial organelle development *in vivo*, long time movies were recorded. After inducing expression of the amphiphilic proteins, cells were set onto an agarose-modified coverslip and imaged by total internal reflection fluorescence (TIRF) microscopy for 5.5 h (see Supplementary Movie 1). The movie illustrates a correlation between the induction of the protein expression and the increase of fluorescent objects over time. Within the first 20 min almost no fluorescent objects could be observed. After approximately 20 min very small fluorescent structures start to appear. The early structures exhibit a highly dynamic movement, which can be described by free diffusion, considering calculated diffusion coefficients (see Supplementary Data 2). With proceeding expression time dynamic and stationary artificial organelles become brighter and grow in size (see Supplementary Data 1) indicating a dynamic correlation between organelle growth and protein expression *in vivo*. In early expression states artificial organelles move very rapidly within the cell and become predominantly stationary and localize predominantly near the pole regions over time.

In vivo live cell imaging of organelle substructures in real time is a challenging task. As a consequence of the technical limits of the method, epi- and normal TIRF fluorescence images cannot resolve and distinguish the detailed structural appearance or localization of the organelles (Supplementary Fig. 1). To characterize and resolve the structural confinement of the artificial organelles *in vivo* and to investigate potential interaction of the organelles with the cytoplasmic membrane in the nanoscopic dimension, a super-resolution microscopy technique was applied (TIRF-structured illumination microscopy (SIM)). Introducing this method is the first step to gain in-depth insight to investigate membrane proteins, interaction processes and protein dynamics close to the interface below the diffraction limit of light. By combining TIRF with SIM, true optical resolution down to 100 nm in the lateral direction can be achieved. This allows the observation of structures below the classical resolution limit for light microscopy (≈ 250 nm), still

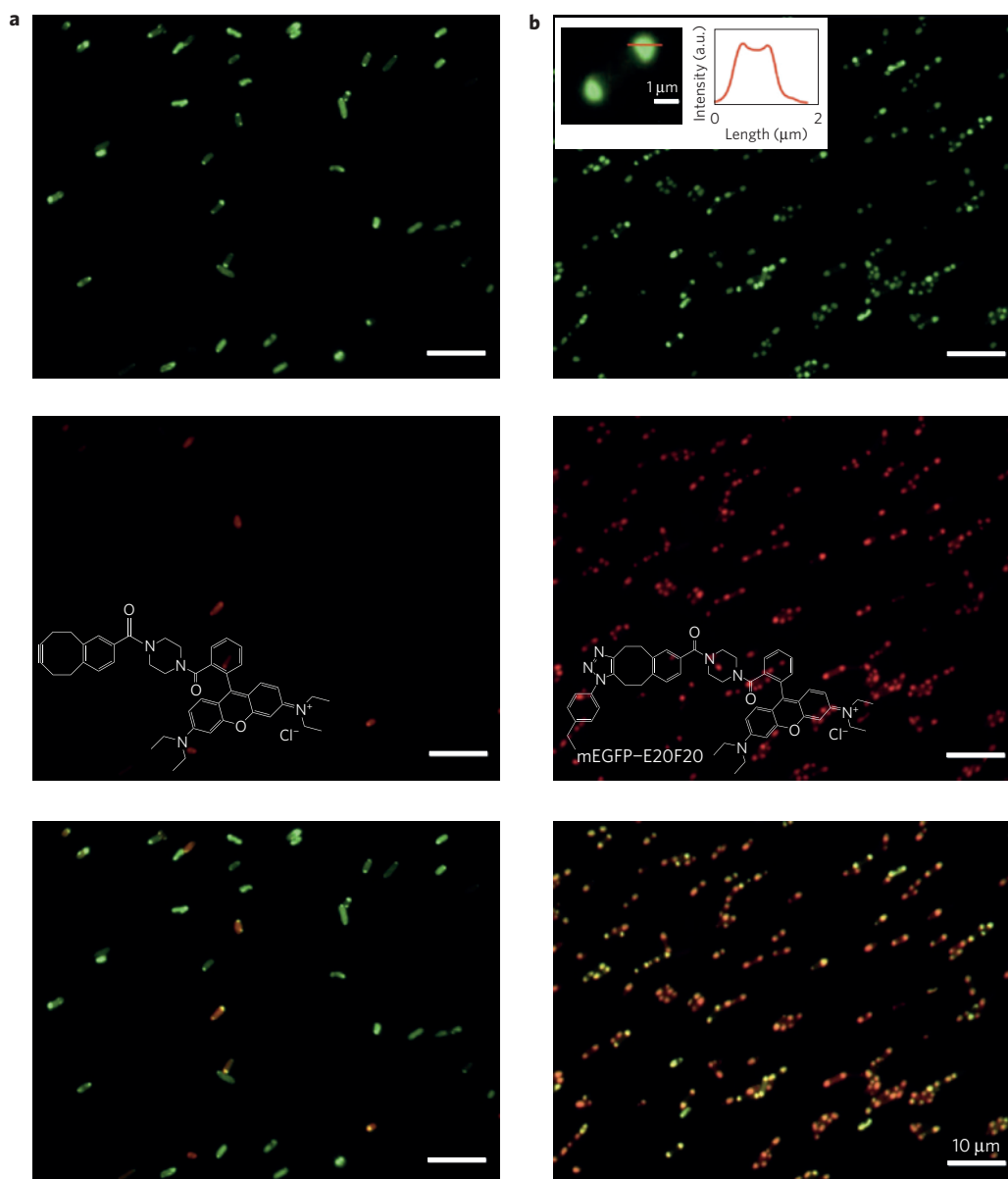


Figure 5 | The site-selective modification of cellular compartments. The organelle-like structures made of pAzF-mEGFP-E20F20 are shown after modification *in vivo* with a fluorescent dye. **a**, *E. coli* cells expressing the mEGFP-E20F20 control protein incubated with azide-reactive COMBO-Rhod dye. Images were taken after multiple washing steps of the cells. Upper panel: GFP signal of the control cells expressing mEGFP-E20F20. Middle panel: the same slide analysed with an RFP (red fluorescent protein) filter. Only a few control cells exhibit a red fluorescent background caused by nonspecifically bound COMBO-Rhod dye. Lower panel: superimposed upper and middle panels. **b**, *E. coli* cells expressing the pAzF-mEGFP-E20F20 protein incubated with COMBO-Rhod dye. Upper panel: GFP signal of the pAzF-mEGFP-E20F20 expressing cells. Middle panel: the red fluorescence demonstrates the successful site-selective modification of the pAzF-mEGFP-E20F20 with COMBO-Rhod dye. Lower panel: superimposed images of upper and middle panels. The inset in the upper panel of **b** illustrates an intensity plot profile of a representative single magnified organelle showing decreased fluorescence in the middle of the vesicle.

benefiting from the high contrast provided by TIRF, which results from the fast axial decay (≈ 170 nm) of the evanescent light field. A set of raw images with illumination grids of different direction and phase is acquired and subsequently reconstructed in a post-processing step³² to yield a super-resolution image with about twofold increased resolution (for details, see Methods). In the normal TIRF image all artificial organelles appear as concentrated fluorescent spots of different size (Fig. 4a). However, in TIRF-SIM a few of the bigger/brighter spots reveal a ring-like substructure with an inner diameter of about 650 nm (Fig. 4b,c). The dark area inside the fluorescent object indicates the close association of the organelle and partial invagination with the cell membrane at the pole

region. This results in a strong decrease of fluorescence excitation for the invaginated part (Fig. 4b,c). The TIRF-SIM observations were verified by TEM images of *E. coli* slices containing artificial organelles, indicating the association, interaction and occasionally a partial invagination of the artificial organelle and the cellular membrane, as represented in Fig. 4d,e and Supplementary Fig. 7b. Similar membrane invaginations and interactions between ELP-coated polystyrene beads and cellular membrane have been reported previously³³. These findings point towards an enhanced interaction potential between some ELPs and the cellular membrane.

Intracellular organelles selectively equipped with enzymes may serve, in the future, as controllable bioreactors, requiring the

precise assembly of several structural and functional elements. A key step towards functional elements could be based on the bio-orthogonal modification of the protein-based artificial organelles inside the living cell. To accomplish this goal we use the site-selective cotranslational incorporation of the unnatural amino acid para-azido-L-phenylalanine (pAzF) in response to the amber stop codon (suppression method)^{34,35}. Thus, we genetically encode a functional group with bio-orthogonal reactivity into the organelle-forming protein. Successful incorporation of pAzF into the amphiphilic protein pAzF-mEGFP-E20F20 was proved by polyacrylamide gel electrophoresis (PAGE; Supplementary Fig. 6) and tandem mass spectrometry (Supplementary Fig. 3). pAzF was introduced close to the N-terminal position at a surface-accessible site and used for bio-orthogonal labelling. The strain-promoted azide-alkyne copper-free cycloaddition³⁶ was applied for the *in vivo* modification of the amphiphilic protein pAzF-mEGFP-E20F20 using the rhodamine dye COMBO-Rhod (ref. 37). For the detailed synthesis of COMBO-Rhod see Supplementary Methods. Artificial organelles composed of the amphiphilic protein pAzF-mEGFP-E20F20 showed strong green and red fluorescence *in vivo*, respectively (Fig. 5b). After protein purification of pAzF-mEGFP-E20F20 red fluorescent gel bands could be detected on the SDS-PAGE gel (Supplementary Fig. 6b). Successful dye modification was confirmed by tandem mass spectrometry (see Supplementary Fig. 3). Controls (mEGFP-E20F20) without pAzF showed only minor unspecific red background fluorescence *in vivo* (Fig. 5a) and on the SDS-PAGE gel (see Supplementary Fig. 6). This is probably a result of the nonspecific association of the charged dye and the amphiphilic protein.

The cotranslational incorporation of an unnatural amino acid allows for the selective addition of chemical, catalytic and biomedical functionalities into the amphiphilic protein *in vivo*. In combination with the genetically controlled expression of the site-selective functionalized amphiphilic protein, the protein-based organelle can be used as a compartment to allow chemical reactions to be constrained within such a nanoreactor³⁸.

We have introduced a synthetic biology approach using amphiphilic protein building blocks, which can be programmed (under genetic control), to make artificial organelles *in vivo*. It is shown that non-lipid molecules can form organelles, enclosed by dynamic membranes, *in vivo*. Not yet functionally embedded within the cell's structural and functional networks, these organelles can introduce additional functions, for example, by introducing multi-enzyme cassettes. The genetic design of the ratio of hydrophilic versus hydrophobic domains within one block-domain protein results in control of the molecular composition and, hence, the assembly of artificial organelles *in vivo*. It could be shown that the length of the hydrophobic and the hydrophilic domains, as well as their translational orientation, guides the assembly process and the resultant structures. Thus, the *de novo* synthesis of defined nanoscale block proteins within the cell may allow the assembly of different protein-based architectures in contrast to *in vitro* experiments. TEM measurements indicate the empty and confined spherical structure of the artificial organelles *in vivo*. Nanoscale interactions of the *de novo* organelles with the membrane of the host cell are observed using TIRF-SIM, a spectroscopic method suitable for the investigation of interfacial processes in living systems below the diffraction limit of light. *In vitro* assembly of the artificial organelles based on pure amphiphilic mEGFP-E20F20 demonstrates that these protein-based building blocks are solely capable of assembling into vesicular compartments. The defined functionalization of these organelles is shown by the site-selective modification of the organelle-forming protein. A fluorescent dye could be conjugated to the site-specifically incorporated unnatural amino acid by copper-free click chemistry *in vivo*. Addressing the physiological effects of the formed organelles within *E. coli* cells,

we show that the assembled organelles did not impede cell viability more than other heterologously expressed protein controls^{39,40} (Supplementary Fig. 5).

The system has potential for many applications, for example, metabolic regulation through substrate channelling¹⁴, where enzymes or metabolites are spatially arranged within the artificial organelles and may allow the reaction turnover to be increased and the prevention of toxic side effects. Applying the new organelles for the coexpression, modulation and functional incorporation of membrane proteins opens up routes to express and study this important class of proteins. Preliminary results of the coexpression of the organelle-forming protein and the heparin-binding epidermal growth factor indicate a membrane protein-organelle co-localization within the living cell (Supplementary Table 2) and *in vitro* (data not shown). Its *de novo* implementation into the cellular context may pave the road to evolutionary experiments enabling the cell to functionally 'code' these organelles allowing the study of the development of new function *in vivo*. Furthermore, block-domain protein-based molecules with defined immiscible blocks will allow the formation of materials with defined inner nanostructures, for example, chiral gyroid phases enabling strategies towards biologically based metamaterials.

Methods

For this study several amphiphilic protein diblock copolymers were constituted *de novo*. The DNA template blocks for the artificial protein domains were generated, assembled and sequenced in a modified pET28 vector as described (Supplementary Methods) before⁴¹. The homopolymeric protein domains were composed of ELP sequence motifs. The hydrophilic domains consist of multiples of the amino-acid sequence motif VPGEG and the hydrophobic block of multiples of the VPGFG motif. These tectons were combined with amphiphilic and non-amphiphilic artificial protein sequences investigated in this study supplemented with fluorescent protein domains: mEGFP-E20F10, mEGFP-E20F20, mEGFP-E20F40, mEGFP-E20F60, F20E20-mEGFP, mEGFP-E40F20, F20E40-mEGFP, mEGFP-E40, mEGFP-E60, E40-mEGFP, E60-mEGFP, E20F20 and E20F10. For the *in vivo* and *in vitro* experiments proteins were expressed in *BLR (DE3)* and in *ER2566 E. coli* cells through isopropyl- β -D-thiogalactoside induction. For details, see Supplementary Information.

The *in vivo* localization and distribution of the artificial proteins were visualized using epifluorescence microscopy with a NIKON eclipse TS100-F fluorescence microscope and a GFP-filter set-up. For further structural characterization of the fluorescent higher-order structures *in vivo* TIRF-SIM images were acquired on an inverted microscope (Leica DM-IRBE). This set-up can monitor the temporal and spatial development of the evolving fluorescent structures within the living cell.

To elucidate the 3D arrangement of the artificial proteins, protein-expressing cells were fixed, stained, polymer embedded and cut into 55 nm slices with a Leica Ultracut EM UC6 microtome⁴². Slices were imaged with an EM Philips CM 100 TEM microscope.

For the *in vitro* vesicle assembly mEGFP-E20F20 was expressed and His-tag purified. Protein purity was confirmed with SDS-PAGE and the buffer was subsequently exchanged by GE Healthcare Minitrapp G25 columns to suitable pH conditions. Proteins were assembled at 25° for 2 h and transferred on a glow-discharged carbon-coated copper grid and negatively stained with 2% uranylformate. TEM measurements were performed on a Zeiss LEO 912 Omega 120 kV. For the *in vivo* modification of the artificial organelles cell cultures expressing pAzF-mEGFP-E20F20 and mEGFP-E20F20 controls were centrifuged, washed three times and resuspended in PBS pH 7.4. After incubation with COMBO-Rhod dye for 2.5 h and a washing step, cells were imaged *in vivo* with a NIKON eclipse TS100-F fluorescence microscope and fluorescence was monitored in the gel band of an SDS-PAGE gel. For mass analysis SDS-PAGE gel bands were cut out and trypsin digested to detect the dye modification using tandem mass spectrometry (for details, see Supplementary Information).

Received 31 March 2014; accepted 22 September 2014;
published online 2 November 2014

References

- Shively, J. M., Decker, G. L. & Greenawalt, J. W. Comparative ultrastructure of the thiobacilli. *J. Bacteriol.* **101**, 618–627 (1970).

2. Shively, J. M., Ball, E., Brown, D. H. & Saunders, R. E. Functional organelles in prokaryotes: Polyhedral inclusions (carboxysomes) of *Thiobacillus neapolitanus*. *Science* **182**, 584–586 (1973).
3. Yeates, T. O., Kerfeld, C. A., Heinhorst, S., Cannon, G. C. & Shively, J. M. Protein-based organelles in bacteria: Carboxysomes and related microcompartments. *Nature Rev. Microbiol.* **6**, 681–691 (2008).
4. Kerfeld, C. A., Heinhorst, S. & Cannon, G. C. Bacterial microcompartments. *Annu. Rev. Microbiol.* **64**, 391–408 (2010).
5. Cheng, S., Liu, Y., Crowley, C. S., Yeates, T. O. & Bobik, T. A. Bacterial microcompartments: Their properties and paradoxes. *BioEssays* **30**, 1084–1095 (2008).
6. Roodbeen, R. & Van Hest, J. C. M. Synthetic cells and organelles: Compartmentalization strategies. *BioEssays* **31**, 1299–1308 (2009).
7. Parsons, J. B. *et al.* Synthesis of empty bacterial microcompartments, directed organelle protein incorporation, and evidence of filament-associated organelle movement. *Mol. Cell* **38**, 305–315 (2010).
8. Vargo, K. B., Parthasarathy, R. & Hammer, D. A. Self-assembly of tunable protein suprapstructures from recombinant oleosin. *Proc. Natl Acad. Sci. USA* **109**, 11657–11662 (2012).
9. Kim, W., Thévenot, J., Ibarboure, E., Lecommandoux, S. & Chaikof, E. L. Self-assembly of thermally responsive amphiphilic diblock copolypeptides into spherical micellar nanoparticles. *Angew. Chem. Int. Ed.* **49**, 4257–4260 (2010).
10. Bellomo, E. G., Wyrsta, M. D., Pakstis, L., Pochan, D. J. & Deming, T. J. Stimuli-responsive polypeptide vesicles by conformation-specific assembly. *Nature Mater.* **3**, 244–248 (2004).
11. Martín, L., Castro, E., Ribeiro, A., Alonso, M. & Rodríguez-Cabello, J. C. Temperature-triggered self-assembly of elastin-like block co-recombinamers: The controlled formation of micelles and vesicles in an aqueous medium. *Biomacromolecules* **13**, 293–298 (2012).
12. Agapakis, C. M., Boyle, P. M. & Silver, P. A. Natural strategies for the spatial optimization of metabolism in synthetic biology. *Nature Chem. Biol.* **8**, 527–535 (2012).
13. Medema, M. H., van, R. R., Takano, E. & Breitling, R. Computational tools for the synthetic design of biochemical pathways. *Nature Rev. Microbiol.* **10**, 191–202 (2012).
14. Dueber, J. E. *et al.* Synthetic protein scaffolds provide modular control over metabolic flux. *Nature Biotechnol.* **27**, 753–759 (2009).
15. Medema, M. H., Breitling, R., Bovenberg, R. & Takano, E. Exploiting plug-and-play synthetic biology for drug discovery and production in microorganisms. *Nature Rev. Microbiol.* **9**, 131–137 (2011).
16. LeDuc, P. R. *et al.* Towards an *in vivo* biologically inspired nanofactory. *Nature Nanotech.* **2**, 3–7 (2007).
17. Israelachvili, J. N. *Intermolecular and Surface Forces* 3rd edn (Academic Press, 2011).
18. Cho, Y. *et al.* Hydrogen bonding of β -turn structure is stabilized in D₂O. *J. Am. Chem. Soc.* **131**, 15188–15193 (2009).
19. Kurková, D. *et al.* Structure and dynamics of two elastin-like polypentapeptides studied by NMR spectroscopy. *Biomacromolecules* **4**, 589–601 (2003).
20. Dreher, M. R. *et al.* Temperature triggered self-assembly of polypeptides into multivalent spherical micelles. *J. Am. Chem. Soc.* **130**, 687–694 (2008).
21. Lee, T. A. T., Cooper, A., Apkarian, R. P. & Conticello, V. P. Thermo-reversible self-assembly of nanoparticles derived from elastin-mimetic polypeptides. *Adv. Mater.* **12**, 1105–1110 (2000).
22. Urry, D. W. *et al.* Elastin: A representative ideal protein elastomer. *Phil. Trans. R. Soc. Lond. B* **357**, 169–184 (2002).
23. Lee, S. C., Choi, Y. C. & Yu, M.-H. Effect of the N-terminal hydrophobic sequence of hepatitis B virus surface antigen on the folding and assembly of hybrid β -galactosidase in *Escherichia coli*. *Eur. J. Biochem.* **187**, 417–424 (1990).
24. Cabrita, L. D., Dobson, C. M. & Christodoulou, J. Protein folding on the ribosome. *Curr. Opin. Struct. Biol.* **20**, 33–45 (2010).
25. Vanhecke, D., Graber, W. & Studer, D. in *Methods in Cell Biology* Vol. 88 (ed. Allen, T. D.) 151–164 (Academic Press, 2008).
26. Hurbain, I. & Sachse, M. The future is cold: Cryo-preparation methods for transmission electron microscopy of cells. *Biol. Cell* **103**, 405–420 (2011).
27. McDonald, K. & Auer, M. High-pressure freezing, cellular tomography, and structural cell biology. *BioTechniques* **41**, 137–143 (2006).
28. Walde, P., Wick, R., Fresta, M., Mangone, A. & Luisi, P. L. Autopoietic self-reproduction of fatty acid vesicles. *J. Am. Chem. Soc.* **116**, 11649–11654 (1994).
29. Shimamoto, T. *et al.* The NhaB Na⁺/H⁺ antiporter is essential for intracellular pH regulation under alkaline conditions in *Escherichia coli*. *J. Biochem.* **116**, 285–290 (1994).
30. Record, M. T. Jr, Courtenay, E. S., Cayley, D. S. & Guttman, H. J. Responses of *E. coli* to osmotic stress: Large changes in amounts of cytoplasmic solutes and water. *Trends Biochem. Sci.* **23**, 143–148 (1998).
31. Chen, I. A. & Walde, P. From self-assembled vesicles to protocells. *Cold Spring Harb. Perspect. Biol.* **2** (2010).
32. Hirvonen, L., Wicker, K., Mandula, O. & Heintzmann, R. Structured illumination microscopy of a living cell. *Eur. Biophys. J.* **38**, 807–812 (2009).
33. Dash, B. C. *et al.* Tunable elastin-like polypeptide hollow sphere as a high payload and controlled delivery gene depot. *J. Control. Release* **152**, 382–392 (2011).
34. Chin, J. W. *et al.* Addition of p-Azido-L-phenylalanine to the genetic code of *Escherichia coli*. *J. Am. Chem. Soc.* **124**, 9026–9027 (2002).
35. Wang, L., Brock, A., Herberich, B. & Schultz, P. G. Expanding the genetic code of *Escherichia coli*. *Science* **292**, 498–500 (2001).
36. Laughlin, S. T., Baskin, J. M., Amacher, S. L. & Bertozzi, C. R. *In vivo* imaging of membrane-associated glycans in developing zebrafish. *Science* **320**, 664–667 (2008).
37. Varga, B. R., Kállay, M., Hegyi, K., Béni, S. & Kele, P. A non-fluorinated monobenzyocyclooctyne for rapid copper-free click reactions. *Chem. Eur. J.* **18**, 822–828 (2012).
38. Schreiber, A. & Schiller, S. M. Nanobiotechnology of protein compartments: Steps towards nanofactories. *Bioinsp. Biomim. Nanobiomater.* **4**, 157–164 (2013).
39. Baneyx, F. Recombinant protein expression in *Escherichia coli*. *Curr. Opin. Biotechnol.* **10**, 411–421 (1999).
40. Glick, B. R. Metabolic load and heterologous gene expression. *Biotechnol. Adv.* **13**, 247–261 (1995).
41. Huber, M. C. *et al.* Introducing a combinatorial DNA-toolbox platform constituting defined protein-based biohybrid-materials. *Biomaterials* **35**, 8767–8779 (2014).
42. Schrand, A. M., Schlager, J. J., Dai, L. & Hussain, S. M. Preparation of cells for assessing ultrastructural localization of nanoparticles with transmission electron microscopy. *Nature Protocols* **5**, 744–757 (2010).

Acknowledgements

We thank R. Thomann for *in vitro* TEM images and the element-specific imaging and high-contrast imaging measurements. For the LC-MS/MS analysis we thank M. Samalikova and J. Dengjel. We are grateful to P. G. Schultz, TSRI, La Jolla, California, USA for providing the plasmid pEVOLpAzF. P.K. acknowledges the financial support of the Hungarian Scientific Research Fund (OTKA, grant numbers K-100134, NN-110214) and the 'Lendület' Program of the Hungarian Academy of Sciences (LP2013-55/2013) is greatly acknowledged. We are grateful to the Freiburg Institute for Advanced Studies (FRIAS), the Institute for Macromolecular Chemistry, the Institute for Pharmaceutical Sciences, the Institute for Micro System Engineering (IMTEK), the competence network of functional nanostructures (KFN), the Baden-Württemberg Stiftung, the Ministry of Science, Research and the Arts (MWK) Baden-Württemberg, the German Science Foundation (DFG): SPP1623 and EXC 294 BIOS Centre for Biological Signalling Studies, the BMBF (BMBF Forschungspreis 2014) and the Rectorate of the University of Freiburg for support.

Author contributions

S.M.S. conceived the project. A.S. performed the *in vitro* and *in vivo* characterization of the newly cloned proteins and their formed structures using fluorescence microscopy and TEM. Further, A.S. conducted the bio-orthogonal modification of the artificial organelles *in vivo*. M.C.H. designed and cloned the different protein constructs, and carried out the coexpression experiments and *in vivo* characterization using fluorescence microscopy. A.S. and M.C.H. contributed equally to the paper. P.v.O. performed the TIRF and TIRF-SIM measurements. P.K. and B.R.V. designed and synthesized the copper-free clickable fluorescent dye. O.K. conducted the HPF experiments. B.J. did the *in vivo* TEM micrographs. S.B. conducted the cryo *in vitro* TEM analysis. All authors discussed the results and commented on the manuscript.

Additional information

Supplementary information is available in the online version of the paper. Reprints and permissions information is available online at www.nature.com/reprints. Correspondence and requests for materials should be addressed to S.M.S.

Competing financial interests

The authors declare no competing financial interests.